

Potential of Nuclear MHD Electric Power Systems

GEORGE R. SEIKEL* AND LESTER D. NICHOLS†
NASA, Lewis Research Center, Cleveland, Ohio

MHD generators are uniquely capable of fully exploiting advances in high-temperature reactor technology for electric power generation. Extension of NERVA technology could make 2500°K long-life, inert, gas-cooled reactors feasible. Such reactors and MHD generators mate into attractive multi-Mw electric power systems for either space or ground applications. A turbo-MHD system using a turbine driven compressor is the most attractive cycle. It has high-cycle efficiency and low-radiator area and temperature for space applications. A space-power system with 10 Mw electric output, shielded for manned missions, could achieve specific masses of 3.5 to 5 kg/kw_e. A ground power station with 60% efficiency also appears feasible.

Introduction

THE NERVA program has resulted in major advances in the technology of high-temperature reactors. As discussed by Holman and Way,¹ long-life, inert, gas-cooled reactors with 2500°K outlet temperatures may be on the horizon of feasibility. The high-temperature capability of MHD systems gives them an inherent advantage over turbo-electric power systems in exploiting this high-temperature reactor technology.

MHD generators are potentially efficient only at multi-Mw power levels. Shielded reactor specific masses, also, improve with higher power level. Thus, MHD generators and nuclear reactors naturally mate into attractive multi-Mw electric power systems. These nuclear-MHD systems would be attractive both for manned electric-propulsion missions and for terrestrial applications.

Various thermodynamic cycles can be considered for MHD power systems. In the authors' opinion, the most attractive cycle is the combined turbo-MHD cycle (Fig. 1). A schematic of the components of this cycle is shown in Fig. 2. This cycle is similar to that considered recently by Bohn et al.² and Millionschikov³ for nuclear-MHD, ground-power stations.

The proposed turbo-MHD cycle uses recuperators, an inner cooled compressor, and turbine reheat to improve the cycle efficiency. The total turbine output is used to drive the compressors. As indicated in Figs. 1 and 2, the working fluid is heated in a reactor to a top temperature T_{MAX} . The fluid then adiabatically expands through an MHD generator which extracts the useful electric power. The fluid then flows through the hot sides of the turbine reheater and high-temperature recuperator, enters the first turbine at a temperature T_{TURB} , is expanded, reheated to T_{TURB} , expanded through the second turbine, and flows through the hot side of the low-temperature recuperator. The fluid is then cooled (in the primary cooler) down to the compressor inlet temperature T_{COMP} . The flow is compressed in three intercooled stages and is then preheated before entering the reactor in the cold sides of the low and high-temperature recuperators.

This study examines the performance of this turbo-MHD cycle and compares it with the equivalent Brayton MHD and Brayton turbo-electric cycles. These various space power systems are compared on the basis of cycle efficiency, radiator area, compressor power, and component temperatures. The

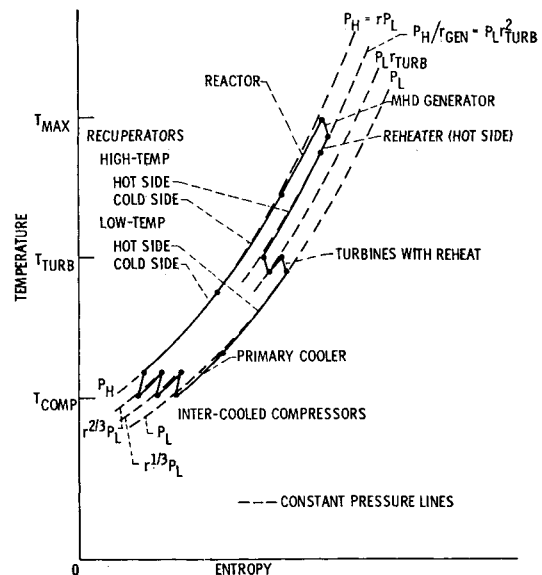


Fig. 1 Turbo-MHD cycle.

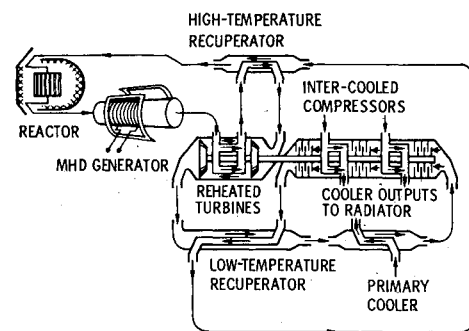


Fig. 2 Turbo-MHD power system.

efficiency of the turbo-MHD system is also calculated for ground power plants. Lastly, the specific masses of 10 Mw man shielded turbo-MHD electric space power systems are estimated.

Cycle Assumptions

For the MHD cycles, a top temperature of 2500°K is assumed and two working fluids are considered: cesium seeded neon and xenon seeded neon. The cesium seed gives the best

Presented as Paper 71-638 at the AIAA/SAE 7th Propulsion Joint Specialist Conference, Salt Lake City, Utah, June 14-18, 1971; submitted July 9, 1971; revision received January 5, 1972.

Index categories: Spacecraft Electric Power Systems; Plasma Dynamics and MHD; Electric Power Generation Research.

* Chief, Plasma Physics Branch. Member AIAA.

† Head, Plasma Power Generation Section.

Table 1 Assumed cycle component performance

Turbine efficiency, η_{TURB}	90%
Compressor efficiency, η_{COMP}	88%
High-temperature recuperator heat loss	5%
Turbine reheater heat loss	5%
MHD generator efficiency, η_{GEN}	
Cesium seed	80%
Xenon seed	55%

possible electrical conductivity and should yield an MHD generator efficiency of 80%. The xenon seed gives a completely inert working fluid but a lower generator efficiency, 55%. For the cycles with turbines, two turbine inlet temperatures are considered: 1500° and 1250°K.

Piping and heat exchanger friction losses are accounted for by assuming that the fractional pressure drops ($\delta = \Delta p/p$) are equal in each nearly constant pressure process of the cycles. The MHD generator efficiency η_{GEN} is defined as the ratio of the electric power output P_e to the power that would be produced in an isentropic expansion through the generator expansion ratio, $1/(1 - \delta)r_{\text{GEN}}$. The turbine efficiency η_{TURB} and expansion ratio $1/(1 - \delta)r_{\text{TURB}}$ are assumed equal for both turbines. The over-all cycle compression ratio r is defined as the ratio of the compressor outlet pressure P_H to the turbine (MHD generator for all MHD cycles) outlet pressure P_L . All cycles considered use three stage intercooled compressors. Each stage is assumed to have the same inlet temperature, compression ratio, and efficiency (η_{COMP}).

For the turbine reheater and the high-temperature recuperator in the turbo-MHD cycle, a fraction of the total thermal power being transferred is assumed lost. The low-temperature recuperator in all cycles has an effectiveness of η_r . In most practical systems, all the coolers in the cycles would most likely be gas to liquid heat exchangers. However, for simplicity, no temperature drop has been accounted for between the gas working fluid and a final heat sink (for space systems the radiator). The assumed values for the performance of the cycle components are summarized in Table 1.

Efficiency of Turbo-MHD Ground Power Station

For a turbo-MHD ground power station, the compressor inlet temperature T_{COMP} is equal to the available heat-sink temperature 300°K. This would correspond to the temperature of ambient cooling water. An air cooled convector radiator could also be used as a heat sink; however, its temperature would be somewhat higher.

For a given temperature reactor and turbine, the cycle efficiency is a function⁴ of the MHD generator efficiency, the cycle compression ratio, the recuperator effectiveness, and the fractional pressure drop δ .

The parametric variations of the cycle efficiencies of turbo-MHD ground power stations having a reactor temperature of 2500°K and a turbine temperature of either 1500° or 1250°K are shown in Fig. 3.[‡] It indicates how the efficiency varies with each of the cycle parameters. The efficiency is the most sensitive to the generator efficiency and the recuperator effectiveness. The crossing of the two turbine temperature curves as a function of η_r results from the fact that for each recuperator effectiveness there is an optimum turbine temperature. Figure 3 shows that an over all cycle efficiency of 60–70% should be obtainable with a 2500°K turbo-MHD ground power station.

[‡] In Fig. 3, the dashed lines indicate common conditions: $\eta_{\text{GEN}} = 80\%$, $\eta_r = 0.9$, $r = 3.33$, $\delta = 1\%$; temperatures are turbine inlet.

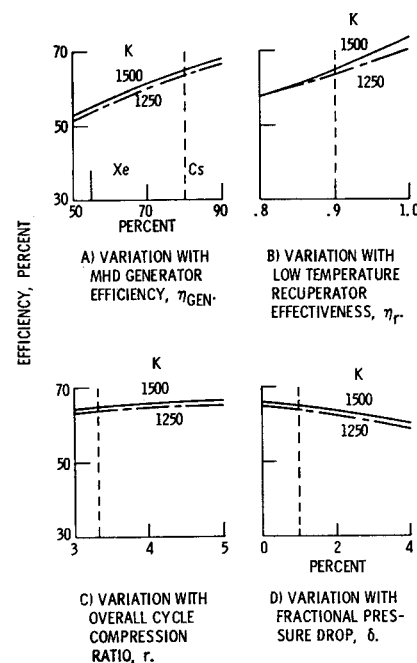


Fig. 3 Parametric variation of over-all cycle efficiency of a 2500°K turbo-MHD ground power station.

Performance of Space Power Systems

For a space power system the compressor inlet temperature is adjusted to obtain the minimum specific radiator area (radiator area divided by the output electric power). This minimum value of specific radiator area decreases with decreasing fractional pressure drop, δ . However, the low-temperature recuperator specific area increases with decreasing fractional pressure drop (because of reduced heat transfer). This recuperator area and δ can be related⁴ by using Reynold's analogy if appropriate turbulent friction factor, compressor outlet pressure, and other properties of the gas are assigned. The values used herein are given in Table 2.

Figure 4 shows the minimum specific radiator area as a function of cycle efficiency for turbo-MHD space power systems having a specific recuperator area of 0.374 m²/kw, turbine-inlet temperatures of 1250° or 1500°K, and MHD generator efficiencies of 80% (cesium seed) or 55% (xenon seed). Also shown in Fig. 4 are the equivalent curves for all MHD cycles with cesium and xenon seeds, i.e., cycles in which the compressor is driven by an electric motor which is powered by part of the output of the MHD generator. Also shown in the figure is a curve for a turboelectric power system with a reactor outlet temperature of 1500°K. A 1250°K turboelectric system was also considered, but it is off the scale of Fig. 4.

A summary of the cycle parameters for that system and the other power systems shown in Fig. 4 for the absolute minimum specific radiator area points is given in Table 3. Table 3 shows that the most attractive features of the turbo-MHD space power system are 1) the high-cycle efficiency, 2) the relatively low-radiator area, 3) the relatively low-radiator temperature compared to the high-performance, all-MHD system, 4) the low ratio of compressor power to net

Table 2 Quantities used to evaluate recuperate area

Compressor outlet pressure, P_H	10 atm
Recuperator friction factor, f	0.003
Ratio of specific heats, γ	5/3
Prandtl number, N_{PR}	0.714

Table 3 Cycle parameters for minimum radiator area space power systems. Low-temperature recuperator specific area, $0.374 \text{ m}^2/\text{kW}_e$.

Cycle Seed	All MHD		Turbo-MHD		All Turbine			
	Cs	Xe	Cs	Xe	Cs	Xe
Temperatures, °K								
Reactor outlet	2500	2500	2500	2500	2500	2500	1500	1250
MHD exit	1567	1748	2070	2177	2148	2206
Turbine inlet	1500	1500	1250	1250	1500	1250
Radiator inlet	1144	890	883	874	739	730	713	591
Compressor: exit	1039	675	801	797	661	660	672	559
inlet	802	485	608	586	739	500	514	425
Cycle efficiency, %	21.4	18.7	38.4	30.2	40.4	32.9	22.5	22.6
Specific radiator area, m^2/kW_e	0.0969	0.659	1202	0.1898	1987	0.3184	0.552	1.160
Ratio compressor to net electrical power	3.21	3.16	1.35	1.96	1.12	1.64	3.19	3.18
Fractional pressure drop, δ , %	4	6	0.6	1	0.6	1	6	6
Over-all compression ratio	5	7.7	6.2	7.7	4.4	6.2	5	5.2

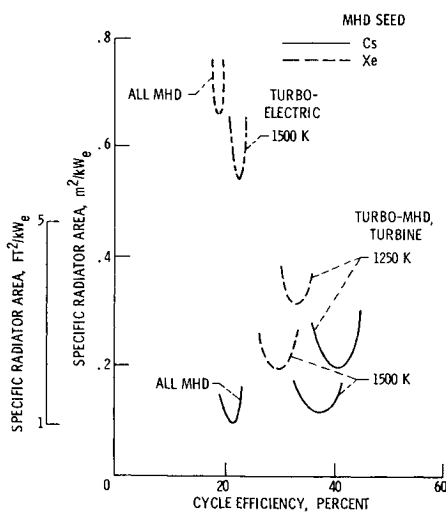


Fig. 4 Specific radiator area as a function of space power system efficiency.

electrical power, 5) the relatively low temperature and pressure ratios required in the MHD generator expansion, and 6) the lower sensitivity of the cycle performance to the MHD generator seed than the all-MHD system.

Specific Mass of 10MW_e Turbo-MHD Space Power System

Reactor Plus Shield

To estimate the mass of the reactor plus shield of a man shielded system the approximate method presented by Moeckel⁵ was used. A cylindrical reactor having an L/D of one and a thermal power density of 100 W/cm^3 was assumed. The two shield configurations shown in Fig. 5 were considered. The first is a 10° included angle shadow shield. The second configuration is a shadow plus peripheral shield. Both shield configurations use an inner tungsten shield to reduce the dose from gamma radiation and an outer lithium hydride shield to attenuate the neutron dose. To make the mass estimates a total dose rate of 10^{-2} rem/hr is assumed at the surface of the shadow shields and a dose rate of 1 rem/hr is assumed at the surface of the peripheral shield. Additional attenuation of these dose rates would occur in practical systems due to both distance and any cabin shielding.

Using the above assumptions and the approximate method of Moeckel one obtains the results shown in Fig. 6 for the

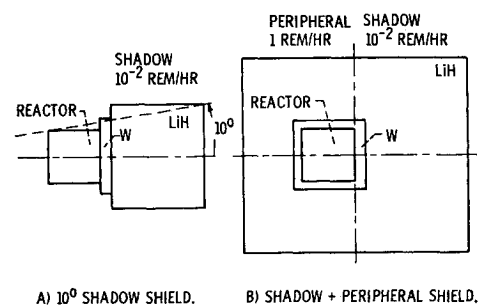


Fig. 5 Reactor and shield configurations.

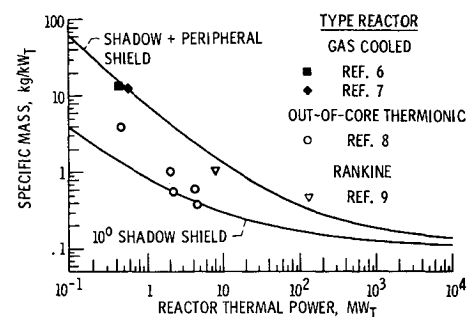


Fig. 6 Specific mass of reactor plus shield.

specific mass of the reactor plus shield as a function of reactor thermal power level. For comparison purposes, also shown in Fig. 6 are a number of specific masses for more detailed man shielded reactor studies.⁶⁻⁹ The open symbols are for shadow shielded reactors and the solid symbols are for reactors designed with both a shadow and a peripheral shield. As indicated in the figure, the approximate method of Moeckel appears to give quite adequate estimates of the reactor plus shield specific mass. This study will use both curves of this figure for estimating reactor plus shield mass.

Radiator

The radiator mass is estimated on the basis of a 8.4 kg/m^2 specific mass. This value was calculated by Haller and Lieblein¹⁰ for a vapor-chamber fin tube radiator for a Rankine power system with a 37.6 m^2 radiating area at 945°K . Their radiator makes use of segmented vapor-chamber fins but the tubes and headers are not segmented. The radiator mass breakdown is 18% headers, 53% tubes, and 29% fins.

Analyses such as Ref. 10 would yield substantially higher specific masses for the large ($\sim 10^3 \text{ m}^2$) radiators required herein. This results primarily from the increased armor thickness required for the larger radiators to obtain the same tube and header nonpuncture probability for meteoroid impact. In the authors opinion, to accept such a specific mass penalty for large radiators is not realistic. If the vapor chamber fin segments of a large radiator were constructed identically to those of Ref. 10, then the probable percent surviving (i.e., not penetrated by meteorites) would not vary with radiator size and the probable statistical deviation would decrease for larger radiators. By also segmenting the tubes and headers of a large radiator, their percent contribution to the radiator mass should easily be maintained at the 71% calculated for the smaller radiator of Ref. 10. Johnsen¹¹ indicates how segmenting the tubes of a tube fin radiator lowers its mass. The authors opinion is therefore that the radiator specific mass (8.4 kg/kw) assumed for this study may be pessimistic since it is based on a radiator with good fin design but with tubes and headers that may be heavier than required. The radiators required herein, also, may be lighter because of their lower temperature.

Other Components

The other components considered in making a system mass estimate are the low-temperature recuperator, the magnet plus MHD generator, and the turbine compressor. The masses of the high-temperature recuperator and the reheater are not considered because they have a large ΔT between the hot and cold sides of the heat exchanger ($> 300^\circ \text{K}$), they should, thus, be much lighter than the low-temperature recuperator.

The mass of a low-temperature recuperator was estimated on the basis of its area and an assumed specific mass per unit area. The specific mass per unit area used herein is 3 kg/m^2 . This would correspond to constructing the recuperator heat-transfer surfaces with 15 mill steel. This specific mass per unit area is consistent with that analyzed by Freedman.⁷

The mass of the magnet plus MHD generator was assumed to be 0.45 kg/kw_e (1 lb/kw_e). This mass estimate appears to be reasonable based upon the technology of megawatt combustion generators and their superconducting magnets.¹²

The mass of the turbine plus compressor is estimated on the basis of the total compressor power times a specific mass per unit compressor power. This specific mass is assumed to be 0.45 kg/kw ($\sim 3/4 \text{ lb/hp}$) of compressor power.

Total System Mass

With the above assumptions the total system masses of the turbo-MHD space power systems can be estimated if one assumes a low-temperature recuperator specific area and the electric power output. However, the resulting masses of the recuperator and the radiator are respectively increasing and decreasing functions of the recuperator specific area. Thus, to evaluate the mass of the four turbo-MHD cycles fairly the

Table 4 Cycle parameters for turbo-MHD space-power systems with minimum radiator plus low-temperature recuperator mass

Seed	Cs	Xe	Cs	Xe
Temperatures, °K				
Reactor outlet	2500	2500	2500	2500
MHD exit	2019	2169	2071	2203
Reheater hot side exit	1678	1828	1817	1947
Turbines: inlet	1500	1500	1250	1250
exit	1176	1176	1008	1007
Radiator inlet	860	862	726	725
Compressors: inlet	564	564	494	493
exit	781	781	655	655
High-temperature recuperator	1097	1095	937	937
cold side inlet				
Reactor inlet	1266	1406	1476	1599
Cycle efficiency, %	38.9	30.3	41.9	33.0
Specific area, m^2/kw_e				
Radiator	.1465	.2136	.2280	.3333
Low temperature recuperator	.1726	.2517	.2111	.3026
Ratio compressor power to electric power	1.35	1.97	1.13	1.64
Over-all compression ratio	8.33	8.33	6.37	6.45
Fractional pressure drop, δ , %	1.35	1.95	1.3	1.33

specific area of the recuperator was chosen for each case so as to minimize the total mass of the recuperator plus radiator. The resulting parameters for the various cycles are tabulated in Table 4.

The total masses were then estimated for 10 Mw_e space power systems using the four turbo-MHD cycles of Table 4. The component and total specific mass for the four cycles, each with the two shielding configurations, are listed in Table 5. The total specific masses of these power systems are all quite low. As indicated previously, they have relatively low-radiator areas and high-cycle efficiency. They are, thus, potentially very attractive space power systems, and would lead to attractive electric rockets for future manned planetary exploration or other high-payload missions.

Conclusions

Although technical feasibility questions regarding nuclear MHD systems remain, the advances in very high-temperature, gas-cooled reactors and the encouraging results being obtained in closed loop MHD generator experiments substantially increase the prospects for these systems. For space power applications, these MHD systems would be attractive for electric propulsion. The resulting electric rockets, if mated with a nuclear rocket booster, would have a total mission time under a year for manned Mars landing missions. For terrestrial applications, these nuclear-MHD systems would be attractive for two types of systems. If cooling water is used as a heat sink, then the MHD systems high efficiency (60–70%) would lower by a factor of three the heat

Table 5 Specific mass of 2500°K, 10 Mw turbo-MHD space-power systems

Shield Turbine temperature, °K	10° Shadow				Shadow and peripheral			
	1500		1250		1500		1250	
Seed	Cs	Xe	Cs	Xe	Cs	Xe	Cs	Xe
Specific mass, kg/kw _e								
Reactor plus shield	0.61	0.73	0.57	0.68	1.93	2.15	1.87	2.07
Radiator	1.23	1.79	1.92	2.80	1.23	1.79	1.92	2.80
Low temperature recuperator	0.52	0.76	0.63	0.91	0.52	0.76	0.63	0.91
MHD generator and magnet	0.45	0.45	0.45	0.45	0.45	0.45	0.45	0.45
Turbines and compressors	0.61	0.89	0.51	0.74	0.61	0.89	0.51	0.74
Total	3.42	4.62	4.08	5.58	4.74	6.04	5.38	6.97

rejection per kw_e of present nuclear power generators. Alternatively, a cycle efficiency of perhaps 45% could be obtainable with these MHD systems using only an air-cooled convector radiator as a heat sink. Such a power source would require no cooling water and might minimize the power plant's effect on the local ecology.

Development of the proposed nuclear turbo-MHD power system will require significant progress in the technology of MHD generators, super-conducting magnetic systems, and high-temperature reactors. Present technology programs are aimed at establishing the feasibility of both the generators^{13,14} and magnets,¹² but have not yet been expanded to explore in depth the feasibility and characteristics of the required very high-temperature reactors.

References

- ¹ Holman, R. R. and Way, S., "Exploring a Closed Brayton Cycle MHD Power System Applying NERVA Reactor Technology," AIAA Paper 70-1225, Houston, Texas, 1970.
- ² Bohn, T., Komarek, P., and Noack, G., "Aspects of Essential Components of Nuclear MHD Plants," *Eleventh Symposium on Engineering Aspects of Magnetohydrodynamics*, California Inst. of Technology, March 24-26, 1970, pp. 109-118.
- ³ Millionschikov, M. D., Lyn'ka, A. U., Nedospasov, A. V., and Shendlin, A. E., "The Possibilities of Using Gas-Turbine Units and Magnetohydrodynamic Generators in Atomic Power Plants with High Temperature Gas Cooled Reactors," *High Temperature*, Vol. 8, No. 2, March-April, 1970, pp. 353-363.
- ⁴ Nichols, L. D., "A Combined Turbine-MHD Brayton Cycle for Space and Ground Use," TN D-6513, 1971, NASA.

⁵ Moeckel, W. E., "Propulsion Systems for Manned Exploration of the Solar System," TM X-1864, 1969, NASA.

⁶ Anon. "The NERVA Technology Reactor Integrated with NASA Lewis Brayton Cycle Space Power System," WANL-TNR-225, May 1970, Westinghouse Electric Corp., Pittsburgh, Pa.

⁷ Freedman, S. I., "Study of Nuclear Brayton Cycle Power System," GE-65SD4251, NASA CR-54397, Aug. 1965, General Electric Co., Philadelphia, Pa.

⁸ Loewe, W. E. "Analysis of an Out-of-Core Thermionic Space Power System," *IEEE Transactions on Aerospace and Electronic Systems*, Vol. AES-5, No. 1, Jan. 1969, pp. 58-65.

⁹ Zipkin, M. A., "Alkali-Metal, Rankine-Cycle Power Systems for Electric Propulsion," *Journal of Spacecraft and Rockets*, Vol. 4, No. 7, July 1967, pp. 852-858.

¹⁰ Haller, H. C. and Lieblein, S., "Analytical Comparison of Rankine Cycle Space Radiators Constructed of Central, Double, and Block-Vapor-Chamber Fin-Tube Geometries," TN D-4411, 1968, NASA.

¹¹ Johnsen, R. L., "Weight Study of Partially Segmented Direct-Condensing Radiators for Large Space Power Systems," TND-3227, 1966, NASA.

¹² Stekly, Z. J. J., Thome, R. J., and Cooper, R. F., "Characteristics of MHD Generator Systems Using Superconducting Field Coils," *Proceedings of the Fifth International Conference on Magnetohydrodynamic Electrical Power Generation* Vol. 4, April 1971, pp. 7-25.

¹³ Sovie, R. J. and Nichols, L. D., "Results Obtained in the NASA-Lewis Closed Cycle Magnetohydrodynamic Power Generation Experiments," TM X-2277, 1971, NASA.

¹⁴ "Closed Cycle Power Generation Experiment," *Closed Cycle Plasma MHD Systems, Proceedings of the Fifth International Conference on Magnetohydrodynamic Electrical Power Generation*, Sec. 2.6, Vol. 2, 1971, pp. 371-496.

MAY 1972

J. SPACECRAFT

VOL. 9, NO. 5

Atomization and Mixing Characteristics of Gas/Liquid Coaxial Injector Elements

R. J. BURICK*

Rocketdyne/North American Rockwell Corporation, Canoga Park, Calif.

The results of a cold-flow characterization study of the mixing and atomization characteristics of several gas/liquid circular coaxial elements are discussed. Mixing and atomization data are presented which show the effect of element geometry as well as element operating conditions. The studies were conducted in unique pressurized facilities in order that hot-fire injector dynamics could be modeled. Local values of gas and liquid mass flux are presented which qualitatively and quantitatively show the mixing quality of the two-phase spray fields. Single parameter correlations for both the mixing and atomization data were obtained. The atomization experiments produced drop size distributions that correlated with the normalized Rosin-Rammler distribution function.

Introduction

THIS paper presents the results of the initial phase of an experimental program (NAS3-12051) to characterize the circular coaxial injector concept for gas/liquid rocket motor applications. The primary objective of the effort was to establish high performance and associated design

criteria for the propellant combination of gaseous methane/liquid FLOX (82.6% F₂, 17.4% O₂) at chamber pressures on the order of 500 psia.

In general, gas/liquid coaxial injector element concepts consist of a central liquid (usually oxidizer) jet which is surrounded by an annulus of high-velocity gas (usually fuel). In this study both the geometric and operating variables of the coaxial element were systematically investigated to determine their effects on the mixing and atomization characteristics of the element.

To establish the required design criteria for full-scale gas/liquid coaxial injectors, an investigation utilizing single-element injectors was conducted. This approach involved the determination of both the propellant mixing and atomization characteristics of coaxial elements using cold-flow

Presented as Paper 71-672 at the AIAA/SAE 7th Propulsion Joint Specialist Conference, Salt Lake City, Utah, June 14-18, 1971; submitted June 22, 1971; revision received December 20, 1971. This work was performed for NASA Lewis Research Center, under Contract NAS3-12051. The author is indebted to J. T. Sabol and D. E. Zwald for assisting in the experimental studies.

* Member of the Technical Staff, Advanced Programs. Member AIAA.